

Quantum computation using NMR

Kavita Dorai[†], T. S. Mahesh[†], Arvind[‡] and Anil Kumar^{†,*,#}

[†]Department of Physics, Indian Institute of Science, Bangalore 560 012, India

[‡]Department of Physics, Guru Nanak Dev University, Amritsar 143 005, India

*Sophisticated Instruments Facility, Indian Institute of Science, Bangalore 560 012, India

This article reviews recent work done by us on some initial steps towards the implementation of quantum computation using liquid state NMR. We describe how special kinds of states required for such computation (called pseudo-pure states) can be created from a thermal ensemble of spins. We demonstrate the implementation of several quantum logic gates through one- and two-dimensional NMR methods, using transition- and spin-selective pulses. Finally, we discuss the implementation of the Deutsch–Jozsa algorithm using NMR.

ALL present-day computations use two-state binary logic and have led to a large revolution in data processing and manipulation. However, several scientists have wondered if quantum mechanical systems could provide a new paradigm for computation. Feynmann in particular, hypothesized that it might be possible to simulate quantum evolution efficiently, provided the simulator was itself quantum-mechanical in nature¹.

The question that arises is: can real quantum systems be used to build computers that operate in the quantum-mechanical regime, and how much more computing power would such devices be able to achieve? These are some interesting issues being addressed by researchers today, and this fusion of ideas from quantum physics and information theory has led to exciting new developments in quantum cryptography^{2,3}, teleportation⁴, error correction^{5,7}, and quantum computation^{8–15}.

It was proved early on, that traditional Boolean logic gates can be implemented using a set of modified ‘reversible’ gates, and that one can find a minimal set of such gates that are sufficient for computation^{16,17}. Furthermore, researchers in the early 1980s made a fundamental connection between quantum mechanics and reversible computation by proposing that reversible Boolean computation can be simulated by the time evolution of a quantum system, which is a unitary reversible dynamic^{18,19}. Logical operations in quantum computation are implemented on quantum bits (qubits), the basic units of quantum information. A qubit can be visualized as the states of a two-level quantum system, like the two spin states of a spin-1/2 particle or the two different polarization states of a single photon. The re-

alization that, the two eigenstates labelled by $|0\rangle$ and $|1\rangle$ can be mapped onto logical 0 and 1, leads to the possibility of the quantum-mechanical implementation of logic gates and circuits^{20–23}. Unlike the classical bit which can exist only in two states, the permitted states for a qubit ($\cos\theta |0\rangle + \sin\theta e^{i\phi} |1\rangle$), span a 2D complex vector space (Figure 1). A state for n qubits can in general be represented by a 2^n -dimensional complex vector. While all classical computation can be performed using the mapping between eigenstates and logical states, the fact that a qubit can exist in a general coherent superposition of the eigenstates, leads to new possibilities for computation. What is intrinsically different about a quantum computation? The answer lies in the fact that it exploits inherently quantum features like quantum superposition and entanglement to solve problems hitherto deemed intractable, on any classical computer. If two qubits are in a state such as $\frac{1}{\sqrt{2}}(|00\rangle - |11\rangle)$, which is not resolvable into the tensor product of the states of the individual qubits, the qubits are said to be entangled^{24–26}. Neither qubit by itself has a definite state, in contrast to a classical system which can be completely resolved into the states of each part of the system. The existence of such entangled states is fundamental to the quantum world and leads to counter-intuitive phenomena like the violation of Bell’s inequalities. It is interesting that such intriguing states have now found an application in computation and information processing, to reduce the level of complexity of computational tasks.

A measure of computational complexity is how the number of steps required for the computation (denoted s) evolves mathematically as a function of the size of the problem (denoted L). If s is a polynomial function of L , the problem is tractable; if s rises exponentially with L , the problem is thought to be intractable^{14,15}. An example of a computationally hard problem is that of the

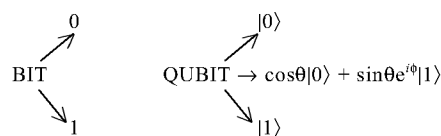


Figure 1. Units of information: bits and qubits. A classical bit can only take the values 0 and 1, whereas a qubit can exist in any coherent superposition of the two.

[#]For correspondence. (e-mail: anilnmr@physics.iisc.ernet.in)

factorization of a number, i.e. to find all the prime factors of a given large integer. Classically, this is known to be computationally intractable since the time taken by the best-known classical algorithm grows exponentially with the size of the input number. This is the security on which most cryptographic systems rely on today. A quantum computer can factor large integers in a time which is polynomial in the logarithm of the best classical time. This brings the non-tractable factoring problem to the domain of tractability and illustrates the true power of quantum computing^{15,27}. In quantum computation, the computation itself can be thought of as a set of unitary transformations U_i acting on a set of input qubits. The main task is to identify suitable quantum systems, prepare them in pure initial states and physically achieve Hamiltonians that generate these unitary transformations, where $U_i = e^{iH_i t}$.

A massive parallelism is achieved in quantum computation, since one is able to perform the computation on all the inputs in one go, by preparing the state of the qubits in a quantum superposition of all the possible classical inputs. However, not all tasks can be speeded up by a uniform amount on a quantum computer – problems like factoring and the simulation of quantum dynamics gain an exponential speed-up, while the database search problem is speeded up polynomially. On the other hand, many problems like inserting an element in an ordered list do not get speeded up at all. The identification of classes of problems that can indeed be solved more efficiently by a quantum computer opens up newer avenues for research. Three path-breaking quantum algorithms in this direction are, the Deutsch–Jozsa (DJ) algorithm to distinguish between two classes of mathematical functions^{28,29}, Shor's quantum factoring algorithm^{27,30}, and Grover's algorithm to rapidly search a database³¹.

The choice of physical systems to build elements of quantum hardware explored thus far, ranges from optical photons^{32,33}, cavity QED^{34,35}, quantum dots³⁶, trapped ions^{37,38} to nuclear spins^{39–42}. As a candidate for quantum computing, NMR is attractive because of the long coherence times exhibited by the spins, and also due to the complexity of logical operations that can be executed on modern spectrometers. A molecule with N spin 1/2 nuclei can be visualized as an N -bit quantum computer, provided the spins are able to interact, one can manipulate their states in a desired fashion and there is a well-defined method of reading out the result of the computation. In the case of liquid-state NMR, one has an ensemble of such N -bit computers with N determined by the number of manipulatable, interacting spins. Quantum computing is usually performed on pure input states, whereas nuclear spins at thermal equilibrium are in a statistical mixture of pure states, with the signal being an average over all the individual states of the ensemble. It has been shown recently that it is pos-

sible to perform quantum computations using special kinds of mixed state ensembles as well (ensembles in pseudo-pure states), and the challenge now is to explore the possibility of carrying out bulk quantum computing using NMR-based information processors.

Previous workers in the field have employed various NMR methods like non-selective pulses, rf gradients, coherence transfer via J -coupling and simultaneous multi-site excitation to create pseudo-pure states^{39,40,43–45}, construct universal quantum logic gates^{46–54} and implement quantum algorithms for two- and three-qubit systems^{55–62}.

In this research account, we demonstrate the utility of transition- and spin-selective pulses in achieving quantum computing using NMR. We exploit the non-commuting nature of operations on connected transitions to prepare the spin system in a pseudo-pure state and execute different logical operations simultaneously⁶³. Different quantum logic gates have been demonstrated using one- and two-dimensional (1D and 2D respectively) NMR techniques. As an illustration of these ideas, we have implemented the DJ quantum algorithm using 1D and 2D schemes. It turns out that a modified version of the DJ algorithm, which uses lesser qubits, brings out its subtle aspects more clearly. The implementation of the algorithm for up to one and two bits does not involve the manipulation of quantum entangled states, and thus finds a classical explanation. It is only for the three-bit case that entangling transformations become essential to solve the problem⁶⁴.

Experiments have been performed at 300 K on Bruker AMX-400 and DRX-500 spectrometers operating at ^1H resonance frequencies of 400 and 500 MHz, respectively. Two, three and four-spin systems have been chosen as qubits for the computation. The T_1 relaxation times in the molecules used, is of the order of a few seconds (3.4–4.6 s), whereas T_2 relaxation occurs within an interval of about 1 second. Selective excitation has been achieved using low power, long duration rectangular-shape and Gaussian-shaped pulses. The lengths of these pulses are tailored to achieve sufficient selectivity in the frequency domain without perturbing the nearest line and hence depends on the magnitude of the smallest J coupling present. The duration of the pulses applied varies from 100 to 263 ms (for J couplings of 9.6 to 3.8 Hz). For small computations, such as the ones performed here, drastic decoherence or dephasing does not occur during the duration of these selective pulses. However, the deleterious effects of such selective pulses must be considered and compensated for, whenever larger computations are attempted.

Creation of pseudo-pure states

Quantum algorithms are usually formulated in terms of pure quantum-mechanical states. The purity of a state

can be best visualized in the ensemble interpretation. A pure state corresponds to an ensemble with each member being described by the same state vector. A mixed ensemble on the other hand, cannot be represented by a single vector in Hilbert space. The density matrix approach has been devised to handle this physical situation, whereby a density operator can be assigned to pure as well as mixed ensembles. Given a pure ensemble with the state vector $|\psi\rangle$, the corresponding density operator $\rho = |\psi\rangle\langle\psi|$ contains all the relevant information about the state. For a mixed ensemble, with say a fraction f members in a state $|\psi\rangle$ and $1-f$ members in state $|\phi\rangle$, the density operator is a statistical mixture of operators corresponding to both the state vectors and is given by $\rho = f|\psi\rangle\langle\psi| + (1-f)|\phi\rangle\langle\phi|$. Therefore, we can always associate a density operator with a general quantum-mechanical system drawn from a general (pure or mixed) ensemble. When the system is in a pure state (drawn from a pure ensemble), it is also possible to assign a state vector to it. A necessary and sufficient condition for the density matrix corresponding to a pure state is $\rho^2 = \rho$. A quantum computer comprising these spins is therefore an ensemble of independent quantum computers, doing the same computation. The initial state of each quantum computer (spin) is randomly determined and the only accessible measurement is an average of all the computers' registers (states of the spins). The result of a computation attempted on this mixed ensemble might get erased by the averaging process over the ensemble. The problem of working with such mixed initial states has been circumvented by creating within the overall density matrix of the system, a subsystem that behaves exactly like a pure state. Such states are termed 'pseudo-pure' states and different schemes to create pseudo-pure states in NMR have been proposed and experimentally implemented^{39,40,43-45,63}.

The preparation of pseudo-pure states from a thermal ensemble involves isolating a sub-manifold of spin states whose transformation properties are similar to those of a pure state. In effect, the excess (or deficit) population of a state among a uniformly populated background of levels, causes it to behave like a pure state. Consider a system of n spins with a 2^n -dimensional Hilbert space. If we now have a state for which all levels except one are equally populated and we are interested in measurements of those operators for which the uniform background (density matrix is a multiple of identity) does not contribute, then for such measurements this state behaves like a pure state, corresponding to the level with excess population. Such states will henceforth be referred to as pseudo-pure states.

At high temperature, the density matrix of an N -spin system is given by

$$\hat{\sigma} = \frac{1}{2^N}(\hat{I} + \beta\hat{\sigma}_\Delta), \quad (1)$$

which consists of a background part proportional to the identity \hat{I} and a traceless, deviation density matrix $\hat{\sigma}_\Delta$. The factor $\beta = \hbar\omega_0/kT$ is very small ($\approx 10^{-6}$) for nuclear spins at room temperature. The identity part of the density matrix does not evolve under rf pulses and does not contribute to the measured NMR signal. After manipulation by rf pulses and/or gradients, the deviation part of the density matrix can be made to behave like a pure quantum state. To illustrate this point, consider a system of two spin-1/2 particles, with the thermal equilibrium density matrix being described by

$$\sigma_{\text{eq}} = \frac{1}{4}\hat{I} + \frac{\beta}{4} \begin{bmatrix} 1 & 0 & 0 & 0 \\ 0 & 0 & 0 & 0 \\ 0 & 0 & 0 & 0 \\ 0 & 0 & 0 & -1 \end{bmatrix}. \quad (2)$$

A small fraction of the spins are in the state describable by $(\sigma_\Delta)_{\text{eq}} = I_{1z} + I_{2z}$; the subscripts 1, 2 label the spins and I_{iz} , etc. are the usual product operator representations of angular momentum vectors⁶⁵. The rest of the spins are in the uniformly populated background and do not contribute to the signal.

Consider now the matrix representation of a traceless deviation density matrix corresponding to the state $I_{1z} + I_{2z} + 2I_{1z}I_{2z}$ is

$$(\sigma_\Delta)_{\text{p-pure}} = \begin{bmatrix} 3/2 & 0 & 0 & 0 \\ 0 & -1/2 & 0 & 0 \\ 0 & 0 & -1/2 & 0 \\ 0 & 0 & 0 & -1/2 \end{bmatrix}. \quad (3)$$

This matrix can be visualized as

$$\begin{aligned} (\sigma_\Delta)_{\text{p-pure}} &= \begin{bmatrix} 2 & 0 & 0 & 0 \\ 0 & 0 & 0 & 0 \\ 0 & 0 & 0 & 0 \\ 0 & 0 & 0 & 0 \end{bmatrix} - \frac{1}{2}\hat{I} \\ &= 2|00\rangle\langle 00| - \frac{1}{2}\hat{I}, \end{aligned} \quad (4)$$

where the identity term does not evolve under rf pulses and is ignored in NMR experiments. This combination of product operators, $I_{1z} + I_{2z} + 2I_{1z}I_{2z}$, hence represents a pseudo-pure state. It is to be noted that the equilibrium density matrix σ_{eq} (eq. (2)) cannot be resolved into two such matrices (one of them being identity) and hence the thermal equilibrium state is not a pseudo-pure state⁴⁰.

Techniques to experimentally prepare pseudo-pure states can be broadly classified as (i) spatial averaging methods which rely on rf gradients for their implemen-

tation⁴⁰, (ii) temporal averaging, where the result of different experiments performed sequentially is time-averaged⁴³ and (iii) logical labelling methods which use manipulations by rf pulses to re-label the states of the spins³⁹.

Spatially averaged pseudo-pure states

A spatially averaged pseudo-pure state can be prepared by a judicious combination of rf gradients and pulses with different flip angles as shown by Cory *et al.*⁴⁰. It is termed spatial since unitary transformations are applied as a function of a spatial degree of freedom. For example, the scheme $[\frac{\pi}{3}]_x^2 - [\Delta]_z - [\frac{\pi}{4}]_x - [\frac{1}{2J}] - [-\frac{\pi}{4}]_y - [\Delta]_z$, where 1, 2 are the spin labels, J the coupling constant, and Δ_z a gradient in the z direction, leads to a final pseudo-pure density matrix represented by $\frac{1}{2}[I_{1z} + I_{2z} + 2I_{1z}I_{2z}]$.

Temporally averaged pseudo-pure states

The temporal averaging technique uses several experiments with different preparation steps, the results of which are averaged to give a pseudo-pure state as demonstrated by Knill *et al.*⁴³. The unitary transformations are performed sequentially in time. As an example, the average of three different experiments P_i , yields a temporally-averaged pseudo-pure state whose density matrix is given by

$$\sigma_{\text{avg}} = \frac{1}{3} \sum_{i=1}^3 P_i \sigma P_i^\dagger. \quad (5)$$

The unitary transformations corresponding to the three experiments are given by

$$P_1 = \begin{bmatrix} 1 & 0 & 0 & 0 \\ 0 & 1 & 0 & 0 \\ 0 & 0 & 1 & 0 \\ 0 & 0 & 0 & 1 \end{bmatrix}; \quad P_2 = \begin{bmatrix} 1 & 0 & 0 & 0 \\ 0 & 0 & 1 & 0 \\ 0 & 0 & 0 & 1 \\ 0 & 1 & 0 & 0 \end{bmatrix}$$

and

$$P_3 = P_2^\dagger. \quad (6)$$

Logically labelled pseudo-pure states

The logical labelling technique to create pseudo-pure states is categorized by the fact that unitary transformations are used to redistribute the populations of states, such that an effective pure state is obtained in the sub-manifold of qubits (spins) to be used for computation,

and ancillary qubits are used as ‘labels’. While the concept underlying the logical labelling method of pseudo-pure state creation has been delineated by Gershenfeld and Chuang³⁹ and Chuang *et al.*⁴¹, there have been very few experimental implementations of such an elegant technique⁴⁵. We have designed novel pulse schemes using transition-selective pulses to create such logically labelled pseudo-pure states⁶³. Consider a three spin-1/2 system (AMX), with the energy levels labelled as in Figure 2. The selective inversion of two unconnected single-quantum transitions of the A spin ($|001\rangle \rightarrow |101\rangle$ and $|010\rangle \rightarrow |110\rangle$) would lead to the creation of a logically labelled pseudo-pure state, with A being the ‘label qubit’ and M, X being the ‘work qubits’ available for computation. The first four eigenstates (labelled by the first spin being in the $|0\rangle$ state) now form a manifold that corresponds to a two-qubit pseudo-pure state, while the last four (labelled by the first spin being in the $|1\rangle$ state) form a different manifold that corresponds to another two-qubit pseudo-pure state. The creation of a pseudo-pure state by this method leads to relative population differences of

$$\begin{bmatrix} 000 & 001 & 010 & 011 & 100 & 101 & 110 & 111 \\ 3/2 & -1/2 & -1/2 & -1/2 & 1/2 & 1/2 & 1/2 & -3/2 \end{bmatrix}. \quad (7)$$

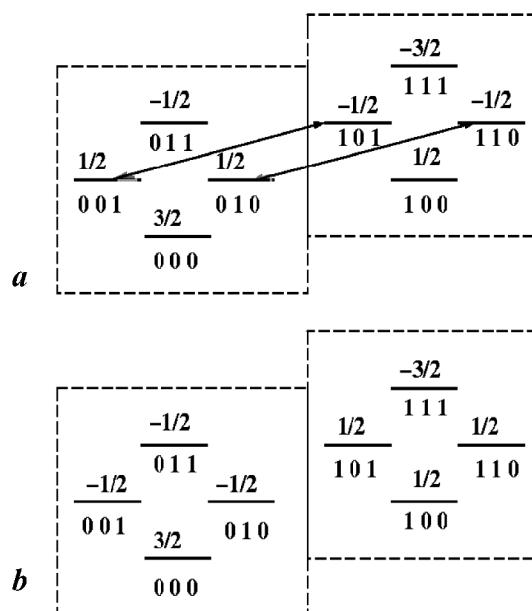


Figure 2. Creation of a pseudo-pure state in a homo-nuclear AMX three-spin system using logical labelling. The energy levels are arranged in increasing order of Larmor frequency with the states of the three spins being labelled as shown below each energy level. The lower (dashed) box encloses states with the first spin (the label qubit) in the $|0\rangle$ state and the upper (dashed) box groups states with the first spin in the $|1\rangle$ state. **a**, Deviation population distribution at the thermal equilibrium is given above each level. **b**, Population distribution of a pseudo-pure state, created by inverting the populations of the two single-quantum A transitions shown in (a) by long arrows.

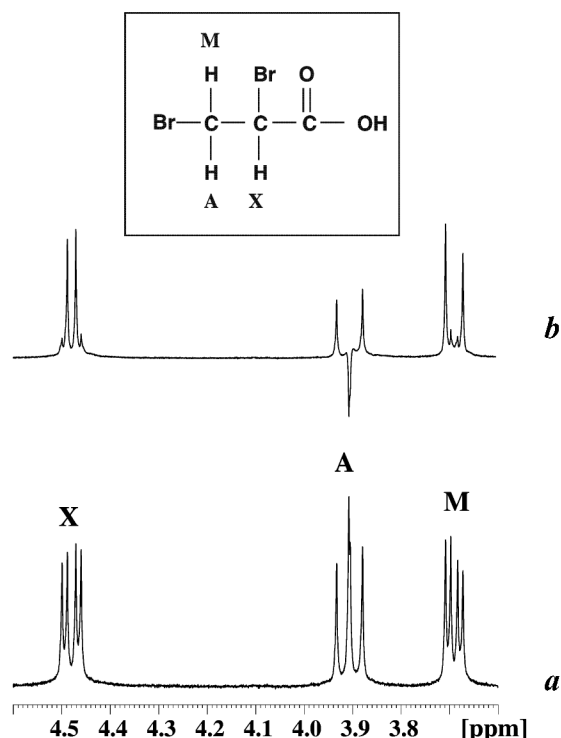


Figure 3. A logically labelled pseudo-pure state in the homo-nuclear three-spin system (AMX) of 2,3-dibromo propionic acid. *a*, Equilibrium proton spectrum with the three protons labelled A, M and X resonating at $\delta_A = 3.91$ ppm, $\delta_M = 3.69$ ppm and $\delta_X = 4.48$ ppm, respectively. *b*, Selective inversion of the two (nearly overlapping) central transitions of the A spin leads to the creation of a logically labelled pseudo-pure state. The selective inversion has been carried out using a long, low-power rectangular π pulse. The state of the spin system has been read by a high-power, small angle (10°) detection pulse.

The experimental creation of a logically labelled pseudo-pure state in the homo-nuclear three-spin system of 2,3-dibromo propionic acid is shown in Figure 3. The pseudo-pure state has been distilled by manipulating unconnected single quantum transitions of the label qubit A, as detailed in eq. (7). A transition-selective π pulse was applied on the two central (nearly overlapping) transitions of the A spin.

Quantum logic gates

A set of two-state systems which evolve under simple unitary operations can be used to implement quantum logic gates and Deutsch proved that one can find a minimal set of gates that are sufficient for computation¹⁷. The action of these gates can be represented by a network diagram and several such gates have been constructed using NMR. One-qubit gates correspond to rotations in the subspace of a single spin, and are easily implemented using spin-selective pulses. The two-qubit quantum XOR (or controlled-NOT) gate has been demonstrated to be fundamental for quantum computation²⁰

and has been implemented in NMR by a selective π pulse on a single transition⁴⁰. The action of the quantum XOR is an evolution under a Hamiltonian that achieves a mapping of two-qubit basis states according to the XOR truth table, i.e. $\{|00\rangle \rightarrow |00\rangle, |01\rangle \rightarrow |01\rangle, |10\rangle \rightarrow |11\rangle, |11\rangle \rightarrow |10\rangle\}$. It has been proved that the reversible quantum XOR gate, supplemented by a set of general one-qubit quantum gates, is sufficient to perform any arbitrary quantum computation²⁰. Various other gates which combine many logical operations might be useful in reducing the number of pulses when larger computations are attempted. We detail the design and experimental implementation of such gates here, using 1D and 2D NMR methods; borrowing from Lewis Carroll, we call such ‘many-in-one’ gates ‘Portmanteau’ gates⁶⁶.

In the 1D method, various transition- and spin-selective pulses have been applied on a two-spin system in equilibrium, to implement different logic gates⁶³. In the context of quantum computing, it was recently recognized by Madi *et al.*⁵¹, that the four stages of a quantum computation (namely initial state preparation, state labelling, computation and readout of result), can be directly related to various steps in two-dimensional NMR (namely preparation, evolution, mixing and detection).

In the two-dimensional method, the states of the ‘computation’ qubits are labelled by the individual transitions of an extra ‘observer’ qubit (instead of being identified by their energy level labels, as is usually the case in one-dimensional experiments). The 2D experiment begins with a $\pi/2$ pulse on the observer spin, which is then allowed to evolve under the free Hamiltonian for a time period t_1 . After the t_1 period, a selective $\pi/2$ pulse on the observer spin restores its magnetization to z-direction, followed by a gradient pulse which destroys unwanted transverse magnetization, if any. The quantum logic gate is then implemented on the computation qubits and the detection of the final state is performed by a spin-selective $\pi/2$ pulse on the observer qubit (Figure 4). The positions of the different multiplet components of the observer spin 2D spectrum, represent the results of the computation.

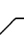
Consider a two-spin system (AX) with each spin being a qubit, the spin A being the first qubit and the spin X, the second qubit. The eigenstates of this system can be represented by $|\epsilon_1, \epsilon_2\rangle$, where ϵ_1 and ϵ_2 are 0 or 1. Various logic operations and portmanteau gates that can be implemented on this two-spin system are categorized in Table 1, along with their truth tables and corresponding unitary transformations. The NOP gate corresponds to a no operation (with no pulses being applied on the qubits).

The SWAP operation

The logical SWAP operation exchanges the states of a pair of qubits. This gate might be useful dur-

Table 1. Characterization of various two-bit logic operations and portmanteau gates. The truth tables and corresponding unitary transformations are given in the different columns

Gate	In	Out	U_f	Circuit diagram
NOP $ \epsilon_1, \epsilon_2\rangle \rightarrow \epsilon_1, \epsilon_2\rangle$	00	00	$\begin{pmatrix} 1 & 0 & 0 & 0 \\ 0 & 1 & 0 & 0 \\ 0 & 0 & 1 & 0 \\ 0 & 0 & 0 & 1 \end{pmatrix}$	
	01	01		
	10	10		
	11	11		
SWAP $ \epsilon_1, \epsilon_2\rangle \rightarrow \epsilon_2, \epsilon_1\rangle$	00	00	$\begin{pmatrix} 1 & 0 & 0 & 0 \\ 0 & 0 & 1 & 0 \\ 0 & 1 & 0 & 0 \\ 0 & 0 & 0 & 1 \end{pmatrix}$	
	01	10		
	10	01		
	11	11		
XOR1 + SWAP + NOT1 $ \epsilon_1, \epsilon_2\rangle \rightarrow \bar{\epsilon}_2, \epsilon_1 \oplus \epsilon_2\rangle$	00	10	$\begin{pmatrix} 0 & 0 & 0 & 1 \\ 0 & 1 & 0 & 0 \\ 1 & 0 & 0 & 0 \\ 0 & 0 & 1 & 0 \end{pmatrix}$	
	01	01		
	10	11		
	11	00		
XNOR2 + SWAP + NOT2 $ \epsilon_1, \epsilon_2\rangle \rightarrow \epsilon_1 \oplus \epsilon_2, \bar{\epsilon}_1\rangle$	00	11	$\begin{pmatrix} 0 & 0 & 1 & 0 \\ 0 & 1 & 0 & 0 \\ 0 & 0 & 0 & 1 \\ 1 & 0 & 0 & 0 \end{pmatrix}$	
	01	01		
	10	00		
	11	10		
NOT + SWAP $ \epsilon_1, \epsilon_2\rangle \rightarrow \bar{\epsilon}_2, \bar{\epsilon}_1\rangle$	00	11	$\begin{pmatrix} 0 & 0 & 0 & 1 \\ 0 & 1 & 0 & 0 \\ 0 & 0 & 1 & 0 \\ 1 & 0 & 0 & 0 \end{pmatrix}$	
	01	01		
	10	10		
	11	00		

The symbol \oplus stands for 'addition modulo 2', while the bar denotes a complement. The symbol  represents the operation NOT. The NOP stands for No Operation, in which no pulse is applied and the unity operator performs no operation.

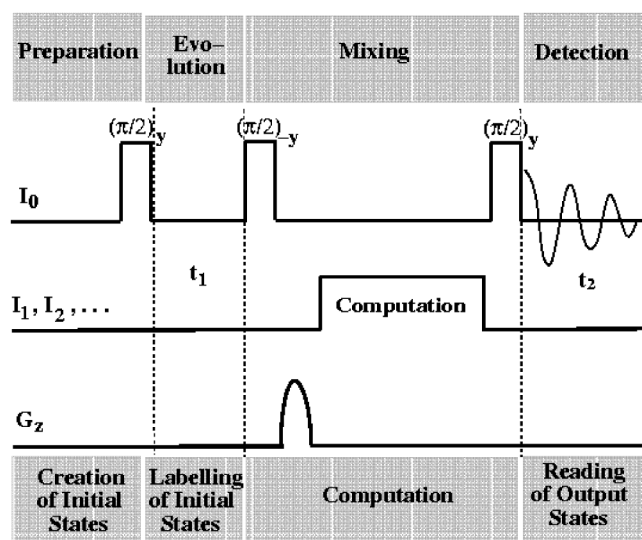


Figure 4. Pulse scheme for quantum computing using two-dimensional NMR. I_0 is the observer qubit and I_1, I_2, \dots are the computation qubits. The gradient pulse G_z eliminates unwanted transverse magnetization before the computation. A two-dimensional data set $s(t_1, t_2)$ is collected, which on double Fourier transform yields a two-dimensional spectrum $s(\omega_1, \omega_2)$. The two-dimensional spectrum correlates the input and output states of the work qubits depending on the computation performed during the mixing/computation period.

ing the course of a computation when qubits need to be permuted⁵⁰. In spin systems where some scalar J couplings are not well resolved, the logical SWAP could be used to compensate for the missing couplings⁵¹. Madi *et al.*⁵¹ have implemented the SWAP operation using an INEPT-type sequence, with non-selective rf pulses and J -evolution. It is interesting to note that the logical SWAP operation can be achieved by selectively interchanging the populations of the zero quantum levels. Since these levels are not connected by single-quantum transitions, the population exchange will have to be achieved indirectly. A pulse sequence to implement this uses transition selective pulses on regressively connected single-quantum transitions, after the creation of a non-equilibrium population distribution⁶⁷. The 1D implementation of the logical SWAP operation achieved by a selective manipulation of the zero-quantum is shown in Figure 5 on the two-spin system of coumarin. The 2D implementation of the SWAP gate is especially interesting and is shown in Figure 6. As discussed earlier, the 1D spectrum of homo-nuclear spins after the execution of a SWAP operation is indistinguishable from that of an equilibrium spectrum and a one-dimensional demonstration of the SWAP gate begins

with the creation of a non-equilibrium state. The 2D method begins with both qubits in the equilibrium state and yields a spectrum characteristic of the SWAP gate.

The 1D implementation of various portmanteau gates on a thermal initial state is shown in Figure 7 for the two-spin system of coumarin. The same pulse schemes will implement the desired logic operations on other initial states (for instance, a pseudo-pure or a coherent superposition of states) as well, without requiring prior knowledge of the state of the system. The implementation of an XOR gate (with the output on the first qubit), followed by a SWAP operation and then a NOT gate on the first qubit can be experimentally achieved by transition-selective π pulses applied consecutively on two progressively connected transitions. Reversing the order of the pulses corresponds to an XNOR + SWAP + NOT gate, with the output on the second qubit. These operations do not commute, so the order in which the pulses are applied is important and its reversal leads to different logical operations. The implementation of a NOT gate followed by a logical SWAP operation (or vice versa, since these operations commute) is achieved by a cascade of transition-selective π pulses on two progressively connected transitions. This tantamounts to a selective inversion of populations of the double-quantum levels.

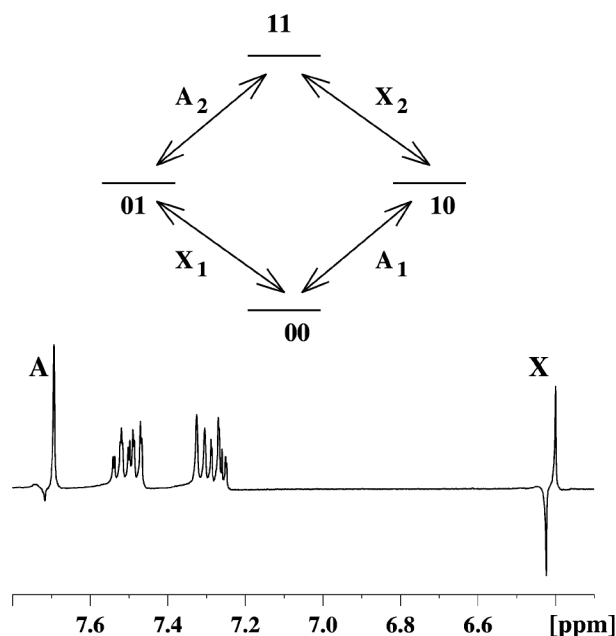


Figure 5. 1D implementation of the logical SWAP operation on the two-spin system of coumarin. The result of the application of a π pulse on one of the X transitions, followed by a π pulse on the regressively connected A transition is shown, which is equivalent to inverting zero quantum using $[A_1]_\pi[X_1]_\pi[A_1]_\pi$ (SWAP operation) preceded by a $[A_1]_\pi$ pulse to create non-equilibrium population distribution. Without this pulse, the 1D spectrum will be indistinguishable from the equilibrium spectrum. A small angle (10°) read pulse has been used. See Figure 7 for the 1D spectrum of coumarin.

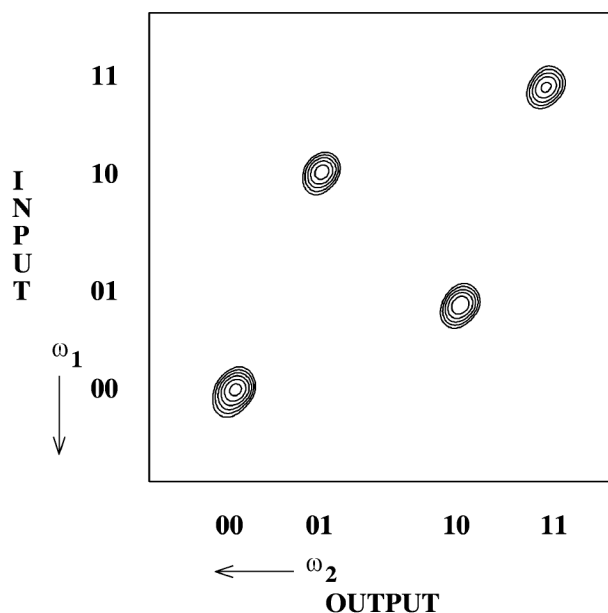


Figure 6. 2D implementation of the logical SWAP operation on the three-spin system of 2,3-dibromo propionic acid, using the pulse scheme of Figure 4. A cascade of non-commuting rectangular/Gaussian transition selective π pulses ($110 \leftrightarrow 111$, $010 \leftrightarrow 011$, $101 \leftrightarrow 111$, $001 \leftrightarrow 011$, $110 \leftrightarrow 111$, $010 \leftrightarrow 011$; see Figure 2 for these transitions) were applied during the computation period. Unlike the 1D case SWAP gate in 2D has been implemented on the equilibrium state, yielding a spectrum characteristic of the SWAP gate.

The 2D implementation of these quantum logic gates on two computation qubits (using an extra observer qubit) is experimentally demonstrated on 2,3-dibromo propionic acid (Figure 8). A complete set (24) of one-to-one reversible 2-qubit gates using two-dimensional NMR on a three-spin system has been carried out⁶⁸. Figure 9 shows several 3-qubit gates implemented on a 4-spin system, using selective pulses. Once again, No Operation during computation period yields NOP gate and inverting spin I_1 yields the NOT (I_1) gate. The more interesting ones are Toffoli gate (or AND/NAND gate) and OR/NOR gate. The operations of Toffoli and OR/NOR gates (13, 15) are respectively,

$$|s, t, u\rangle \rightarrow |s \oplus (t \wedge u), t, u\rangle, \quad (8)$$

and

$$|s, t, u\rangle \rightarrow |s \oplus (t \vee u), t, u\rangle, \quad (9)$$

where $\oplus \equiv$ addition modulo 2, $\wedge \equiv$ AND, $\vee \equiv$ OR and s, t, u are the states of the control spin I_1 and the input spins I_2 and I_3 . The Toffoli gate is a universal gate for reversible computation.

The 1D pulse schemes for the implementation of gates are useful and easy to implement. The advantage of the two-dimensional method is that it correlates the input and output states and thus the readout of the com-

putation is graphic. However, the 2D method requires an extra qubit to encode the computation.

The Deutsch–Jozsa quantum algorithm

The DJ algorithm determines whether an unknown function $f(x)$ is constant or balanced²⁸. The algorithm affords the simplest demonstration of the power of a quantum computer over its classical counterpart. In general, consider an n -bit binary string x ; a Boolean function f can be defined on this n -bit domain space to a 1-bit range space, with the restriction that either the output is the same for all inputs (the function is constant) or the output is 0 for half the inputs and 1 for the other half (the function is balanced). All the 2^n possible input strings are valid inputs for the function ($f(x) = \{0, 1\}$). In quantum computation, these n -bit logical strings are in one-to-one correspondence with the eigenstates of n -qubits, and one can hence label the logical string x by the eigenstate $|x\rangle$. Classically, for an n -bit domain space, one needs to compute the function

at least $2^{n/2} + 1$ times in order to determine whether it is constant or balanced. The DJ algorithm achieves this on a quantum computer using only a single function call.

The usual implementation of the DJ algorithm (the Cleve version²⁹) for n bits requires $n + 1$ qubits, the function f being encoded through an f -dependent unitary transformation,

$$|x\rangle_{n\text{-bit}} |y\rangle_{1\text{-bit}} \xrightarrow{U_f} |x\rangle_{n\text{-bit}} |y \oplus f(x)\rangle_{1\text{-bit}}, \quad (10)$$

where \oplus denotes addition modulo 2. As shown in Figure 10, the implementation of the unitary transformation U_f , along with the Hadamard transformation, then suffices to distinguish the function as constant or balanced^{28,29}. A Hadamard transformation on one qubit mixes the eigenstates maximally,

$$\begin{aligned} |0\rangle &\xrightarrow{H} \frac{1}{\sqrt{2}}(|0\rangle + |1\rangle) \\ |1\rangle &\xrightarrow{H} \frac{1}{\sqrt{2}}(|0\rangle - |1\rangle); H = H^{-1} = \frac{1}{\sqrt{2}} \begin{pmatrix} 1 & 1 \\ 1 & -1 \end{pmatrix}. \end{aligned} \quad (11)$$

The Hadamard transformation for n -qubits is the tensor product of the one-qubit transformation ($H^n = H \otimes H \otimes H \dots \otimes H$), its action on the n -qubit eigen states being

$$H^n |x\rangle = \sum_{y=0}^{2^n-1} (-1)^{\oplus \sum_j x_j y_j} |y\rangle, \quad (12)$$

where x_j and y_j are the j th entries of the n -bit strings x and y .

The four possible functions for the one-bit DJ algorithm (encoded using one extra qubit) are categorized as shown in Table 2.

The unitary transformations corresponding to the four possible propagators U_f are easily constructed:

$$\begin{aligned} U_1 &= \begin{bmatrix} 1 & 0 & 0 & 0 \\ 0 & 1 & 0 & 0 \\ 0 & 0 & 1 & 0 \\ 0 & 0 & 0 & 1 \end{bmatrix}; \quad U_2 = \begin{bmatrix} 0 & 1 & 0 & 0 \\ 1 & 0 & 0 & 0 \\ 0 & 0 & 0 & 1 \\ 0 & 0 & 1 & 0 \end{bmatrix} \\ U_3 &= \begin{bmatrix} 1 & 0 & 0 & 0 \\ 0 & 1 & 0 & 0 \\ 0 & 0 & 0 & 1 \\ 0 & 0 & 1 & 0 \end{bmatrix}; \quad U_4 = \begin{bmatrix} 0 & 1 & 0 & 0 \\ 1 & 0 & 0 & 0 \\ 0 & 0 & 1 & 0 \\ 0 & 0 & 0 & 1 \end{bmatrix}. \end{aligned} \quad (13)$$

We have implemented the DJ algorithm in a 1D and a 2D fashion, using spin-selective and transition-selective π pulses. The experiment begins with both qubits being in a coherent superposition of states $(\frac{|0\rangle \pm |1\rangle}{\sqrt{2}})$. This has been achieved by a non-selective $[\pi/2]_y$ pulse on both spins. After application of the propagators U_i , the first

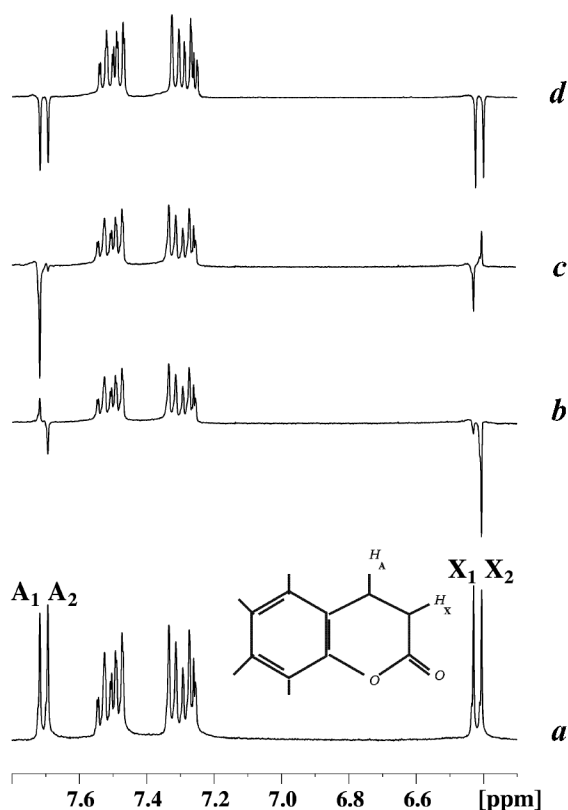


Figure 7. 1D implementation of various portmanteau gates on a two-qubit system. **a**, Reference spectrum of coumarin at thermal equilibrium. This corresponds to the NOP gate. **b**, Implementation of an XOR + NOT + SWAP (by the pulse cascade $[A_1]_\pi[X_2]_\pi$, where A_1 and X_2 refer to progressively connected transitions of spins A and X, respectively). **c**, Implementation of an XNOR + NOT + SWAP ($[X_2]_\pi[A_1]_\pi$). **d**, Implementation of a NOT + SWAP ($[A_1]_\pi[X_2]_\pi[A_1]_\pi$). The state of the spin system is read by a small (10°) angle pulse in each case.

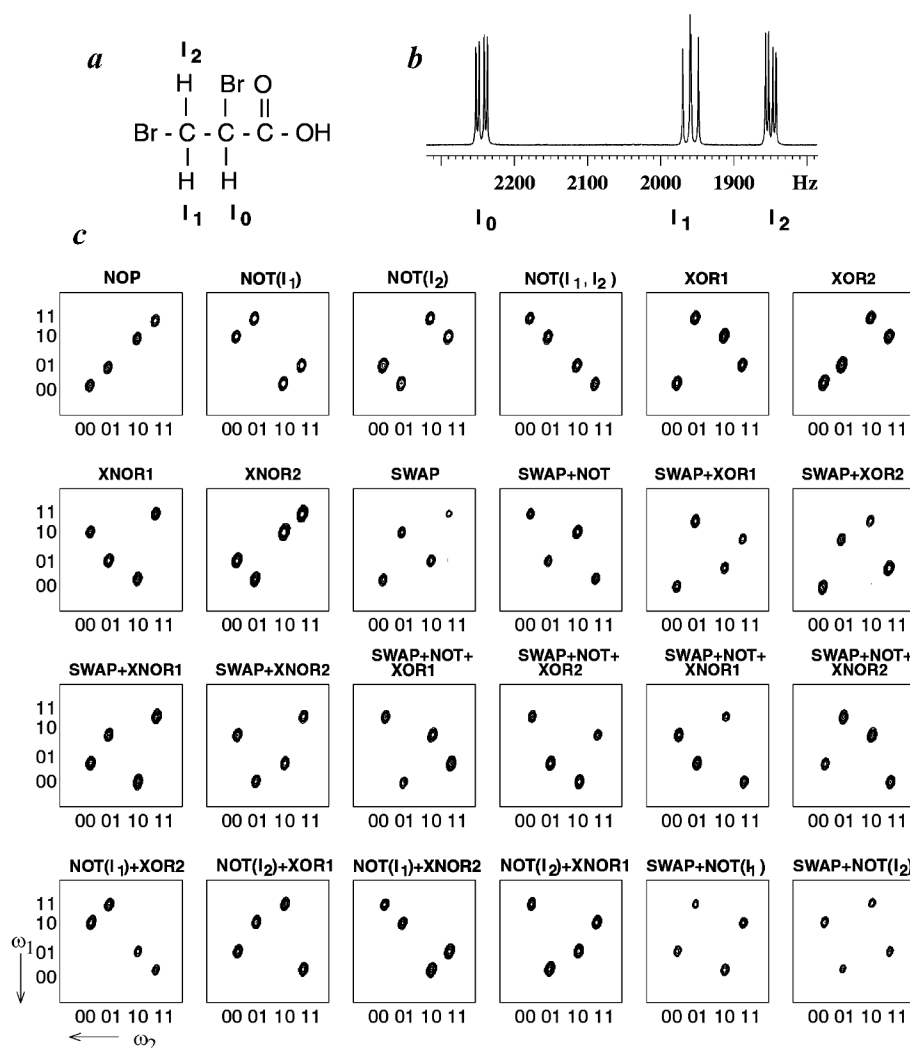


Figure 8. Implementation of a complete set of 24 one-to-one reversible 2D quantum gates on a three-spin system using one observer and two work qubits. **a**, 2,3-dibromo propionic acid; **b**, 1D ^1H NMR spectrum of **(a)** dissolved in CDCl_3 , recorded on a Bruker DRX-500 spectrometer at 300 K; **c**, 2D spectrum of observer spin (I_0), corresponding to various gates implemented using spin- and transition-selective pulses. The computation pulses for each of these gates are given in ref. 68. Low-power rectangular/Gaussian pulses were utilized for various gates. Spin-selective pulses were 10 ms long and the transition-selective pulses were 100–300 ms long. The phase of the computation pulses were cycled through $(x, -x)$ to suppress the distortions due to pulse imperfections. All experiments were carried out in the time domain with 256 t_1 values and 256 complex data points along t_2 and with 2 scans for each t_1 point. Zero filling to 512×512 complex data points was done prior to the 2D Fourier transformation. All plots are shown in magnitude mode.

qubit (the ‘control’ qubit) remains in the superposition state, while the desired result ($f(0) \oplus f(1)$) is encoded as the appearance or disappearance of the lines of the target qubit. The U_1 transformation corresponds to the unity operation or ‘do nothing’, while the U_2 transform is achieved by a spin-selective $[\pi]_x$ pulse on the control qubit. The U_3 and U_4 transformations are implemented by selective π pulses on the $|10\rangle \rightarrow |11\rangle$ and the $|00\rangle \rightarrow |01\rangle$ transitions, respectively.

In a single measurement, one can distinguish between constant and balanced functions on the basis of the disappearance of the lines of the target qubit in the spec-

trum. These predictions are borne out by the experimental spectra in Figure 11. The phase of the transition-selective pulse (used to implement the U_3 and U_4 transformations) has been stepped through $(x, -x, y, -y)$ to suppress phase distortions and leads to the total suppression of the target qubit lines and the retention of only one line of the control qubits. The implementation of the algorithm does not require pure initial states, since similar results can be read out from the spectrum if one starts with thermal initial states instead. The 2D implementation of the DJ algorithm on the same system is shown in Figure 12 (ref. 68).

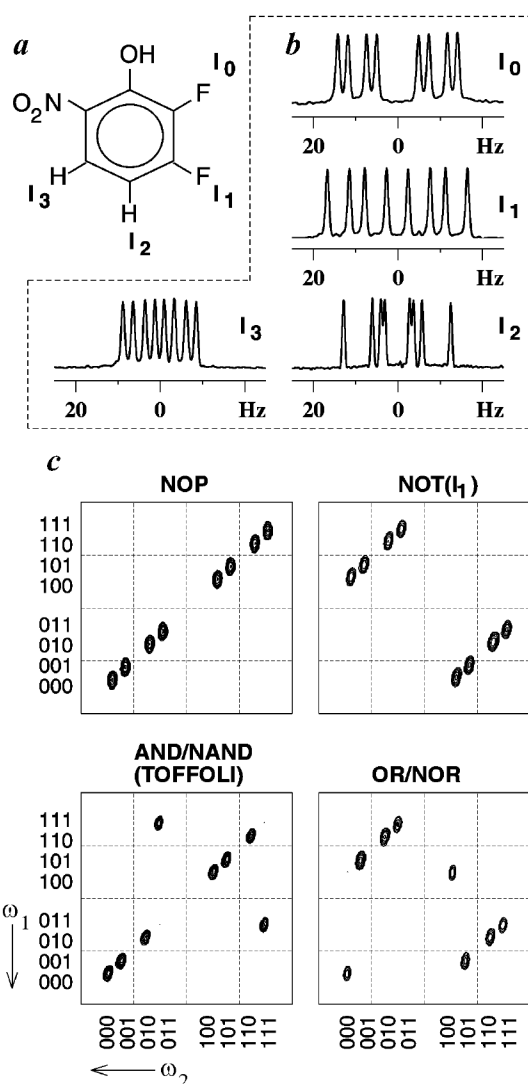


Figure 9. Implementation of 3-qubit 2D gates using ^{19}F and ^1H NMR. *a*, 2,3-difluoro-6-nitrophenol. *b*, ^{19}F and ^1H NMR spectra of (*a*) dissolved in CDCl_3 (with one drop of D_2O to induce the exchange of the hydroxy proton and hence to suppress its coupling to fluorine nuclei) recorded on a Bruker DRX-500 spectrometer at 300 K. *c*, ^{19}F 2D spectra of observer spin I_0 corresponding to various gates. The spin-selective pulses were 1 ms long and the transition-selective pulses were 200 ms long. The NOP gate requires no computation pulse, while the NOT (I_1) uses a selective π pulse on I_1 . The Toffoli gate uses a pair of transition selective π pulses to invert the control spin transitions 011 and 111. The OR/NOR gate uses a spin selective π pulse on the control spin and then a pair of transition selective π pulses on 010 and 110 transitions of the control spin.

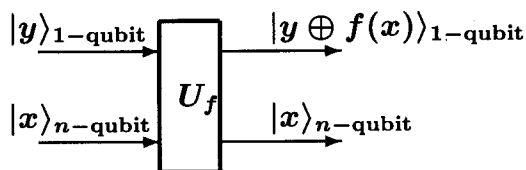


Figure 10. Function call mechanism for the DJ algorithm for n qubits, using $n + 1$ input qubits.

Table 2. Four possible functions for the one-bit DJ algorithm

x	Constant		Balanced	
	f_1	f_2	f_3	f_4
0	0	1	0	1
1	0	1	1	0

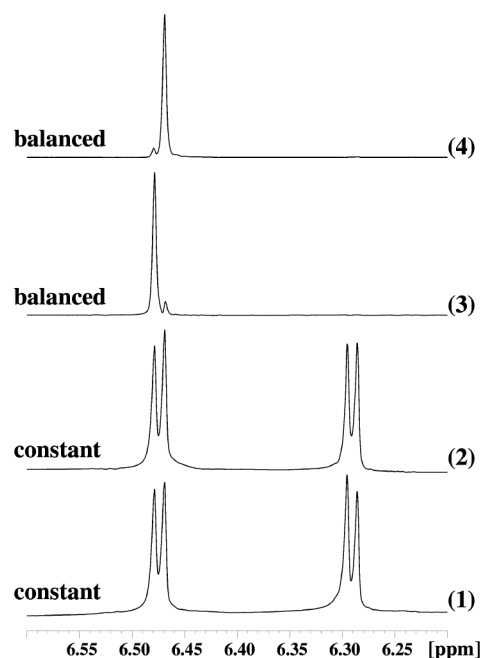


Figure 11. 1D selective pulse implementation of the DJ quantum algorithm on a two-qubit system 5-nitro furfuraldehyde, at room temperature on a 400 MHz spectrometer. The results after applying the unitary transformations U_1 , U_2 , U_3 and U_4 on a coherent superposition are shown in (1), (2), (3) and (4), respectively.

A modified scheme can be designed to solve the n bit Deutsch problem, using n qubits alone⁶⁹. In this scheme, for every function f a unitary transformation is constructed, such that its action on the eigenstates of n -qubits is

$$|x\rangle_{n\text{-bit}} \xrightarrow{U_f} (-1)^{f(x)} |x\rangle_{n\text{-bit}}. \quad (14)$$

Consider n qubits, all in the state $|0\rangle$; a Hadamard transformation H^n converts this state to a linear superposition of all 2^n eigenstates with equal amplitudes and no phase differences. The unitary transformation U_f (defined in eq. (14)) acting on this state, introduces an f -dependent phase factor in each eigenstate in the superposition. At this juncture, all information about f is encoded in the quantum state of the n qubits. A Hadamard transformation H^n is once again applied in order to extract the function's constant or balanced nature.

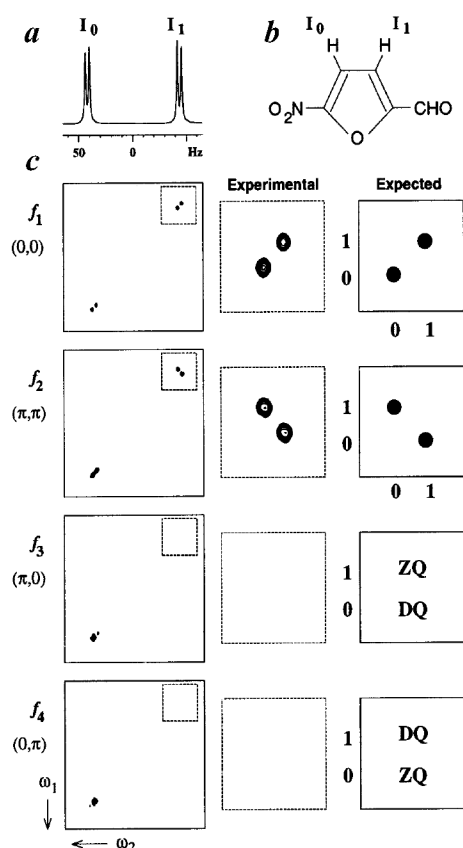


Figure 12. 2D implementation of the DJ algorithm on 5-nitroualdehyde in C_6D_6 on a Bruker DRX-500 spectrometer at 300 K. The 1H spectrum is shown in (a) and the structure of the compound in (b).

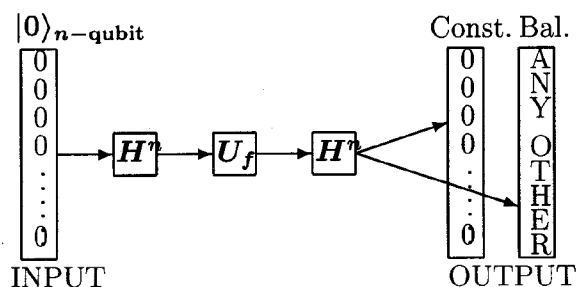


Figure 13. Block diagram for the modified DJ algorithm.

$$|0\rangle \xrightarrow{H^n} \sum_{x=0}^{2^n-1} |x\rangle \xrightarrow{U_f} \sum_{x=0}^{2^n-1} (-1)^{f(x)} |x\rangle \xrightarrow{H^n} \sum_{x=0}^{2^n-1} \sum_{y=0}^{2^n-1} (-1)^{f(x)} (-1)^{\oplus \sum_j x_j y_j} |y\rangle. \quad (15)$$

The final expression for the output state in eq. (15) clearly has an amplitude 1 for the state $|0\rangle_{n\text{-bit}}$ for a constant function and an amplitude 0 for a balanced func-

tion. This categorization of the function as constant or balanced through a single function call using n qubits, is shown pictorially in Figure 13. The number of functions for the n -bit Deutsch problem is $^N C_{N/2} + 2$ (where $N = 2^n$).

The NMR implementation of the modified DJ algorithm for one, two and three qubits, would require the implementation of unitary transformations corresponding to 4, 8 and 72 functions, respectively. This implementation of the DJ algorithm does not require the initial preparation of the spins in a pseudo-pure state, since the thermal equilibrium state serves equally well as a good initial state. The observable spectral result is the same in both cases, though beginning with a pseudo-pure state creates some (undetectable) multiple-quantum coherence. We have implemented the unitary transformations using composite- z pulses, spin-selective pulses and evolution under the scalar J -coupling. We discovered that it is only at the level of three or more input qubits that entangling transformations are essential⁶⁴. The three-qubit DJ algorithm thus affords the simplest example where quantum entanglement plays a definitive role in the computation.

Concluding remarks

This article seeks to give a short account of the state-of-the-art in NMR quantum computing, by demonstrating experimentally various selective pulse and multi-dimensional implementations of pseudo-pure states, novel quantum logic gates and quantum algorithms. In conclusion, we would like to reiterate that NMR is a promising technique to illustrate and explore ideas in quantum computation. The ease with which quantum circuits can be implemented in multi-pulse FTNMR experiments and the facility with which spin dynamics can be manipulated using a variety of techniques is a major advantage. However, one of the challenges for NMR spectroscopists at the moment is to increase the number of qubits available for computation. Efforts are on in this direction, using liquid crystal solvents, labelled nuclei in hetero-nuclear systems, quadrupolar nuclei and even solid-state NMR techniques. We hope NMR will be able to better address current problems in quantum computing such as implementing quantum algorithms with a greater number of qubits, constructing error correcting circuits for fault-tolerant computing, and performing large-scale quantum simulations.

1. Feynmann, R. P., *Int. J. Theor. Phys.*, 1982, **21**, 467.
2. Bennett, C. H., Bessett, F., Brassard, G., Savail, L. and Smolin, J., *J. Cryptol.*, 1992, **5**, 3.
3. Phoenix, S. J. D. and Townsend, P. D., *Contemp. Phys.*, 1995, **36**, 165.
4. Bennett, C. H., Brassard, G., Crepeau, C., Jozsa, R., Peres, A. and Wootters, W. K., *Phys. Rev. Lett.*, 1993, **70**, 1895.

5. DiVincenzo, D. P. and Shor, P. W., *Phys. Rev. Lett.*, 1996, **77**, 3260.
6. Steane, A. M., *Phys. Rev. Lett.*, 1996, **77**, 793.
7. Knill, E. and Laflamme, R., *Phys. Rev. A*, 1997, **55**, 900.
8. DiVincenzo, D. P., *Science*, 1995, **270**, 255.
9. Bennett, C. H., *Phys. Today*, 1995, **273**, 44.
10. Chuang, I. L., Laflamme, R., Shor, P. W. and Zurek, W. H., *Science*, 1995, **270**, 1633.
11. Lloyd, S., *Phys. Rev. Lett.*, 1995, **75**, 4714.
12. Barenco, A., *Contemp. Phys.*, 1996, **37**, 375.
13. Preskill, J., *Proc. R. Soc. London A*, 1998, **454**, 385.
14. Steane, A., *Rep. Prog. Phys.*, 1998, **61**, 117.
15. Bennett, C. H. and DiVincenzo, D. P., *Nature*, 2000, **404**, 247.
16. Deutsch, D., *Proc. R. Soc. London A*, 1985, **400**, 97.
17. Deutsch, D., *Proc. R. Soc. London A*, 1989, **425**, 73.
18. Bennett, C. H., *Int. J. Theor. Phys.*, 1982, **21**, 905.
19. Benioff, P., *Phys. Rev. Lett.*, 1982, **48**, 1581.
20. Barenco, A., Bennett, C. H., Cleve, R., DiVincenzo, D. P. Margolus, N., Shor, P. W., Sleator, T., Smolin, J. A. and Weinfurter, H., *Phys. Rev. A*, 1995, **52**, 3457.
21. DiVincenzo, D. P., *Phys. Rev. A*, 1995, **51**, 1015.
22. Monroe, C., Meekhof, D. M., King, B. E., Itano, W. M. and Wineland, D. J., *Phys. Rev. Lett.*, 1995, **75**, 4714.
23. DiVincenzo, D. P., *Proc. R. Soc. London A*, 1998, **454**, 261.
24. Ekert, A. and Knight, P. L., *Am. J. Phys.*, 1994, **63**, 415.
25. Peres, A., *Phys. Rev. Lett.*, 1996, **77**, 1413.
26. Horodecki, P., *Phys. Lett. A*, 1997, **232**, 333.
27. Shor, P. W., *SIAM J. Comput.*, 1997, **26**, 1484.
28. Deutsch, D. and Jozsa, R., *Proc. R. Soc. London A*, 1992, **439**, 553.
29. Cleve, R., Ekert, A., Macchiavello, C. and Mosca, M., *Proc. R. Soc. London A*, 1998, **454**, 339.
30. Ekert, A. and Jozsa, R., *Rev. Mod. Phys.*, 1996, **68**, 733.
31. Grover, L. K., *Phys. Rev. Lett.*, 1997, **79**, 325.
32. Chuang, I. L. and Yamamoto, Y., *Phys. Rev. A*, 1995, **52**, 3457.
33. Turchette, Q. A., Hood, C., Lange, W., Mabushi, H. and Kimble, H. J., *Phys. Rev. Lett.*, 1995, **75**, 4710.
34. Domokos, P., Raimond, J., Brune, M. and Haroche, S., *Phys. Rev. Lett.*, 1995, **52**, 3554.
35. Sleator, T. and Weinfurter, H., *Phys. Rev. Lett.*, 1995, **74**, 4087.
36. Bandyopadhyay, S. and Roychowdhury, V., *Jpn. J. Appl. Phys.*, 1996, **35**, 3350.
37. Cirac, J. I. and Zoller, P., *Phys. Rev. Lett.*, 1995, **74**, 4091.
38. Steane, A. M., *Appl. Phys. B*, 1997, **64**, 623.
39. Gershenfeld, N. and Chuang, I. L., *Science*, 1997, **275**, 350.
40. Cory, D. G., Fahmy, A. F. and Havel, T. F., *Proc. Natl. Acad. Sci. USA*, 1997, **94**, 1634.
41. Chuang, I. L., Gershenfeld, N., Kubinec, M. G. and Leung, D. W., *Proc. R. Soc. London A*, 1998, **454**, 447.
42. Jones, J. A., LANL preprint, quant-ph/0002085 (2000).
43. Knill, E., Chuang, I. L. and Laflamme, R., *Phys. Rev. A*, 1998, **57**, 3348.
44. Knill, E., Laflamme, R., Martinez, R. and Tseng, C. H., *Nature* 1988, **396**, 52, LANL e-print quant-ph/9908051, 1999.
45. Lieven, M. K. Vandersypen, Yannoni, C. S., Sherwood, M. H. and Chuang, I. L., LANL e-print, quant-ph/9905041, 1999.
46. Cory, D. G., Price, M. D. and Havel, T. F., *Physica D*, 1998, **120**, 82.
47. Cory, D. G., Price, M. D., Maas, W., Knill, E., Laflamme, R., Zurek, W. H., Havel, T. F. and Somaroo, S. S., *Phys. Rev. Lett.*, 1998, **81**, 2152.
48. Laflamme, R., Knill, E., Zurek, W. H., Catasti, P. and Mariappan, S. V. S., *Philos. Trans. R. Soc. London A*, 1998, **356**, 1941.
49. Nielsen, M. A., Knill, E. and Laflamme, R., *Nature*, 1998, **396**, 52.
50. Jones, J. A., Hansen, R. H. and Mosca, M., *J. Magn. Reson.*, 1998, **135**, 353.
51. Madi, Z. L., Bruschweiler, R. and Ernst, R. R., *J. Chem. Phys.*, 1998, **109**, 10603.
52. Price, M. D., Somaroo, S. S., Dunlop, A. E., Havel, T. F. and Cory, D. G., *Phys. Rev. A*, 1999, **60**, 2777.
53. Jones, J. A. and Knill, E., *J. Magn. Reson.*, 1999, **141**, 322.
54. Collins, D., Kim, K. W., Holton, W. C., Sierzputowska-Gracz, H. and Stejskal, E. O., *Phys. Rev. A*, 2000, **62**, 022304/1-4.
55. Jones, J. A. and Mosca, M., *J. Chem. Phys.*, 1998, **109**, 1648.
56. Chuang, I. L., Vandersypen, L. M. K., Zhou, X., Leung, D. W. and Lloyd, S., *Nature*, 1998, **393**, 143.
57. Chuang, I. L., Gershenfeld, N. and Kubinec, M., *Phys. Rev. Lett.*, 1998, **80**, 3408.
58. Jones, J. A., Mosca, M. and Hansen, R. H., *Nature*, 1998, **393**, 344.
59. Jones, J. A., *Science*, 1998, **280**, 229.
60. Linden, N., Barjat, H. and Freeman, R., *Chem. Phys. Lett.*, 1998, **296**, 61.
61. Marx, R., Fahmy, A. F., Myers, J. M., Bermel, W. and Glaser, S. J., *Phys. Rev. A*, 2000, **62**, 012310/1-8.
62. Jones, J. A. and Mosca, M., *Phys. Rev. Lett.*, 1999, **83**, 1050.
63. Dorai Kavita, Arvind and Anil Kumar, *Phys. Rev. A*, 2000, **61**, 042306/1-7.
64. Arvind, Dorai Kavita and Anil Kumar, LANL e-print quant-ph/9909067, 1999.
65. Ernst, R. R., Bodenhausen, G. and Wokaun, A., *Principles of Nuclear Magnetic Resonance in One and Two Dimensions*, Oxford University Press, Oxford, England, 1987.
66. Carroll Lewis, *Through the Looking Glass and What Alice Found There*, Hamlyn House, England, 1871.
67. Dorai Kavita and Anil Kumar, *J. Magn. Reson. A*, 1995, **114**, 155.
68. Mahesh, T. S., Dorai Kavita, Arvind, and Anil Kumar, quant-ph/0006123, 2000.
69. Collins, D., Kim, K. W. and Holton, W. C., *Phys. Rev. A*, 1998, **58**, R1633.

ACKNOWLEDGMENTS. The use of 400 and 500 MHz FTNMR spectrometers of the Sophisticated Instruments Facility (SIF), Indian Institute of Science, funded by Department of Science and Technology, New Delhi is gratefully acknowledged. We also thank Prof. K. V. Ramanathan and Dr G. A. Naganagowda of SIF for useful discussions.

Received 29 August 2000; revised accepted 27 October 2000